Measurement 125 (2018) 11–18

Contents lists available at ScienceDirect

Measurement

journal homepage: www.elsevier.com/locate/measurement

Application of digital shearing speckle pattern interferometry for thermal stress

X. Wang[a], Z. Gao[a,*], S. Yang[a], C. Gao[a], X. Sun[a], X. Wen[a], Z. Feng[b], S. Wang[c], Y. Fan[a]

[a] Key Laboratory of Luminescence and Optical Information of Ministry of Education, Beijing Jiaotong University, Beijing, China
[b] Bradley Department of Electrical and Computer Engineering, Virginia Tech, Blacksburg, VA, USA
[c] Technical University of Munich, Institute for Measurement Systems and Sensor Technology, Theresienstrasse 90/N5, Munich, Germany

ARTICLE INFO

Keywords:
Shearography
Thermal stress
Wavelet transformation
FEM

ABSTRACT

A thermal stress measuring method based on the digital shearing speckle pattern interferometry (DSSPI) is proposed in this paper. The concept of the method is that the thermal inequality leading to the deformation of the object surface will be recorded by the shearing speckle pattern, which is captured by CCD and analyzed in computer subsequently. This system making use of Wollaston prism has obvious advantages in non-contact, instantaneity, high-efficiency, low-cost, robustness and simplicity. The principle of the method is elucidated, and related experimental results with the simulation of finite element method (FEM) in contrast are presented.

1. Introduction

With the development of railway traffic system, the measurement of the thermal stress in continuous welded rail, a significant topic in the maintenance of railway, draws increasing number of attention from different domain. In order to measure the thermal stress with high accuracy and intensity, we have developed and applied a novel optical techniques based on digital shearing speckle pattern interferometry (DSSPI). Compared with traditional method, our system is of advantage in its real-time, full-field and non-destructive measurement.

The existent methods have obvious limitations and imperfection. The traditional methods, such as the electrical resistance strain gauge [1,2], the ultrasonic measurement [3,4] and the Barkhausen noise analysis [5], are limited in many aspects and cannot meet the requirements in practice. For example, in the electrical resistance strain gauge, the measurement is point-by-point and its accuracy is affected by many insecure factors related to the condition on site [6]. Some other techniques, such as digital image correlation [7] and thermoelastic stress analysis [8,9], provide access to full-field measurement [10], but thermoelasticity method needs infrared optical elements and detectors, which are expensive, and compared with the interferometric method, the measuring accuracy of digital image correlation (DIC) method is not high. Furthermore, both of them are directly proportional to the sum of the principal stresses [11] and cannot measure the stresses components.

Regarded as noise of the holography originally, the speckle, which now is the basis of numerous optical techniques on account of its high sensitivity to surface displacements, has been increasingly attracting emphasis and research since 1960s. Among these techniques, Shearography is outstanding, which was built by Hung and Leendertz and developed into DSSPI soon afterwards [12]. For its obvious advantages, DSSPI now has found many significant applications in industrial field, such as the non-destructive testing and the measurement in derivatives of surface displacements.

It proves available to apply speckle interferometry in the measurement of thermal stress [13], but no such system based on DSSPI has been put forward. We have built a shearography measuring system built on Wollaston prims in earlier search [14], and in this paper, we adapt it for measurement of thermal stress. Compared with other shearography method [15], our system gets rid of spatial phase-shift parts and realizes real-time measurement; and this is vital in the measurement under a transient thermal field.

By use of our home-made DSSPI system, we carried out a series of experiments in which artificial thermal loads were applied and compared the result with the simulation of finite element method (FEM). The result of the experiment shows that our system performs very well in the full-field measurement of thermal stress with high accuracy, instantaneity, and reliable structure.

2. Principle

2.1. Thermal stress analysis

When heated, different parts of the track experience different

* Corresponding author.
E-mail address: zhangao@bjtu.edu.cn (Z. Gao).

https://doi.org/10.1016/j.measurement.2018.04.073
Received 26 September 2017; Received in revised form 16 April 2018; Accepted 19 April 2018
Available online 21 April 2018
0263-2241/

heating rates, creating thermal deformations, strain and stress. The deformation is complex and the strain tensor $\boldsymbol{S}$ can be presented as [16]

$$\boldsymbol{S} = \begin{bmatrix} \varepsilon_{xx} & \varepsilon_{xy} & \\ \varepsilon_{yx} & \varepsilon_{yy} & \\ \varepsilon_{zx} & \varepsilon_{zy} & \end{bmatrix} = \begin{bmatrix} \frac{\partial u}{\partial x} & \frac{1}{2}\left(\frac{\partial u}{\partial y}+\frac{\partial v}{\partial x}\right) & \frac{1}{2}\left(\frac{\partial u}{\partial z}+\frac{\partial w}{\partial x}\right) \\ \frac{1}{2}\left(\frac{\partial v}{\partial x}+\frac{\partial u}{\partial y}\right) & \frac{\partial v}{\partial y} & \frac{1}{2}\left(\frac{\partial v}{\partial z}+\frac{\partial w}{\partial y}\right) \\ \frac{1}{2}\left(\frac{\partial w}{\partial x}+\frac{\partial u}{\partial z}\right) & \frac{1}{2}\left(\frac{\partial w}{\partial y}+\frac{\partial v}{\partial z}\right) & \frac{\partial w}{\partial z} \end{bmatrix}, \tag{1}$$

where ε_{ij}, $i,j \in (x,y,z)$, are the values of the strain tensor $\boldsymbol{S}$; u,v,w are the values of displacements in three directions.

An equilibrium equation between strain and stress can be got from basic mechanical relationship [17]

$$\begin{cases} \mu\left(\frac{\partial^2 u}{\partial x^2}+\frac{\partial^2 u}{\partial y^2}+\frac{\partial^2 u}{\partial z^2}\right)+(\mu+\lambda)\left(\frac{\partial^2 u}{\partial x^2}+\frac{\partial^2 v}{\partial x\partial y}+\frac{\partial^2 w}{\partial x\partial z}\right)-\frac{E\alpha}{1-2\nu}\cdot\frac{\partial T}{\partial x}+f_x=0 \\ \mu\left(\frac{\partial^2 v}{\partial x^2}+\frac{\partial^2 v}{\partial y^2}+\frac{\partial^2 v}{\partial z^2}\right)+(\mu+\lambda)\left(\frac{\partial^2 u}{\partial x\partial y}+\frac{\partial^2 v}{\partial y^2}+\frac{\partial^2 w}{\partial y\partial z}\right)-\frac{E\alpha}{1-2\nu}\cdot\frac{\partial T}{\partial y}+f_y=0 \\ \mu\left(\frac{\partial^2 w}{\partial x^2}+\frac{\partial^2 w}{\partial y^2}+\frac{\partial^2 w}{\partial z^2}\right)+(\mu+\lambda)\left(\frac{\partial^2 u}{\partial x\partial z}+\frac{\partial^2 v}{\partial z\partial y}+\frac{\partial^2 w}{\partial z^2}\right)-\frac{E\alpha}{1-2\nu}\cdot\frac{\partial T}{\partial z}+f_z=0 \end{cases}, \tag{2}$$

where σ_{ij}, $i,j \in (x,y,z)$, are the values in the stress tensor, E is the elastic modulus, ν is the Poison ratio, α is the thermal expansion coefficient, T is the temperature, f_x, f_y, f_z are the values of forces per volume, μ and λ are the Lamé coefficients which can be expressed as

$$\mu = \frac{E}{2(1+\nu)}, \lambda = \frac{E\nu}{(1+\nu)(1-2\nu)}. \tag{3}$$

However, there is a traditional assumption, in which the stress is related to the strain with a simpler formula. In some conditions, such as the deformation in a rod-shaped object that is fixed at both ends, it can be assumed that only in one direction occurs the displacement. Considering that assumption, Eq. (2) can be simplified as Hook's law [18]

$$\sigma = E\varepsilon. \tag{4}$$

In other words, by measuring the detectable strain, the stress can be confirmed in a simple way. That is the basis of our method.

2.2. Principle of DSSPI

The schematic of the shearography system we developed to measure out-of-plane displacement is shown in Fig. 1. The object to be measured whose surface is rough enough for the scattering of illuminating light is illuminated with the expanded laser light. The shearing device splits scatting light into two identical but nonparallel beams, which finally meet and intervene with each other at the surface of CCD camera. The CCD is connected to a computer to record, analyze and display the pattern instantly.

The CCD camera can capture the interferometric fringe because the shearing device makes co-linear two light beams scattered from different points on the surface of object. The Wollaston prim is applied in

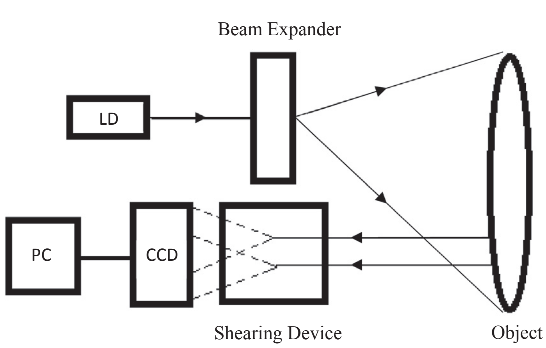

Fig. 1. The shearography system.

our application to replace the Michelson shearing interferometer [14]. Dispensing the shifting parts, this shearing device based on the Wollaston prim has advantages in providing the real-time fringe pattern and allows the immediate phase unwrapping.

When the deformation occurs on the surface of the object due to the mechanical or thermal load, the speckle pattern will change accordingly. The intensity can be described as

$$I = I_0(1+\gamma\cos\varphi), \tag{5}$$

where I is the intensity distribution, I_0 is the background light intensity, γ is the amplitude of modulation of the speckle pattern, φ is the phase changing over time.

By means of recording the patterns during the deformation and subtraction between each patterns, the phase of light field in Eq. (5) can be easily separated out. After per-pixel subtraction, the pattern can provide visible fringe pattern that could be confirmed by

$$I_\Delta = I_0\left[\gamma\sin\left(\varphi_0+\frac{\Delta\varphi}{2}\right)\sin\frac{\Delta\varphi}{2}\right], \tag{6}$$

where φ_0 is the initial constant phase related to spatial distance and $\Delta\varphi$ is the phase difference between the patterns that are inputted in the image subtraction. It is obvious that the intensity of the subtracted patterns is modulated by the temporal function of $\Delta\varphi$, which, as can be seen in Fig. 2(c), produces a butterfly fringe pattern where the dark fringe lines correspond to $\Delta\varphi = 2n\pi$ and the bright fringe lines correspond to $\Delta\varphi = 2(n+1)\pi$ with n the fringe order.

Once the phases are solved out by analyzing the fringe patterns, the deformation derivative can be acquired as well counting on the relationship with phase difference, which can be expressed as [19]

$$\frac{\partial w}{\partial x} = \frac{\Delta\varphi\lambda}{4\pi\Delta x}, \tag{7}$$

where $\partial w/\partial x$ is the out-of-plane displacement derivative, λ is the wavelength of laser and Δx is the distance of two points that interfere with each other on the shearing images, which is merely related with the splitting angle of the Wollaston prism. In the experiments carried out, the wavelength is 532 nm, the Δx is 20 mm and that means the deformation derivative between each order of fringe is about 1.33×10^{-5}. The measurement range of the DSSPI system mainly depends on the instrumentation and the correlation between the speckle patterns., and deformation ranging from a few micrometers to a few hundreds of micrometers can be measured [20].

The intensity is mutable while the deformation results from the transient thermal stress, thus it is significant to realize temporal analysis which is impractical for traditional phase-shifting method due to its inextricable link to clumsy shifting parts. The temporal wavelet translation, as a result of that, is introduced to signal analysis with its advantage in the multi-resolution and localization in the time-or-space-frequency domain [21]. As far as the intensity in Eq. (5) is concerned, the continuous wavelet coefficient can be expressed as

$$W_f(a,b) = |a|^{-\frac{1}{2}}\int I(x,y,t)\cdot\psi^*\left(\frac{t-b}{a}\right)dt, \tag{8}$$

where a is the scale parameter, b is the shift parameter and ψ^* is the mother wavelet. The phases φ and amplitudes A is given by the following expressions [22]

$$A(\mathrm{a,b}) = \sqrt{(\mathrm{Im}(W_f(\mathrm{a,b})))^2+(\mathrm{Re}(W_f(\mathrm{a,b})))^2}, \tag{9}$$

$$\varphi(a,b) = \arctan\left(\frac{\mathrm{Im}(W_f(\mathrm{a,b}))}{\mathrm{Re}(W_f(\mathrm{a,b}))}\right), \tag{10}$$

where $\mathrm{Im}(W_f(\mathrm{a,b}))$ is the imaginary part of $W_f(\mathrm{a,b})$ and $\mathrm{Re}(W_f(\mathrm{a,b}))$ is the real part of $W_f(\mathrm{a,b})$. After being unwrapped, the regional phase obtained from Eq. (10) can be transformed into global phase, and the displacement-derivative in Eq. (7) can be also solved out.